We are IntechOpen, the world's leading publisher of Open Access books Built by scientists, for scientists

6,900
Open access books available

186,000
International authors and editors

200M
Downloads

Our authors are among the

154
Countries delivered to

TOP 1%
most cited scientists

12.2%
Contributors from top 500 universities

WEB OF SCIENCE™

Selection of our books indexed in the Book Citation Index in Web of Science™ Core Collection (BKCI)

Interested in publishing with us?
Contact book.department@intechopen.com

Numbers displayed above are based on latest data collected.
For more information visit www.intechopen.com

Chapter 6

Proteresis of Core-Shell Nanocrystals: Investigation through Theoretical Simulation and Experimental Analysis

Jhong-Yi Ji and Sheng Yun Wu

Additional information is available at the end of the chapter

http://dx.doi.org/10.5772/62398

Abstract

A study of proteresis (inverted hysteresis) in core-shell nanocrystals is presented. A core-shell anisotropic energy (CSAE) model is established to describe the observed proteretic behavior in Ni/NiO core-shell nanocrystals. The magnetic compositions of core-shell nanocrystals can be selected for ferromagnetic, antiferromagnetic, or paramagnetic materials where the exchange intercoupling between them results in both a large effective anisotropic energy and intercoupling energy. Simulation of the magnetization of core-shell nanocrystals reveals the existence of an exchange in the intercoupling energy between the interface of the core and shell moments that, surprisingly, is tuneable in both hysteresis and proteresis. Observations have shown a distinct proteresis, which is related to the spin-flip and exchange intercoupling energy between Ni and NiO. Our approach shows that the processing-dependent technology plays an important role when the grain size decreases to the order of nanometers and when the magnets are reduced from the single domain to core-shell domain. Integrated studies of process-dependent, theoretical modeling and core-shell nanocrystal fabrication technology will lead to more encouraging development in the overunity industry.

Keywords: proteresis, hysteresis, core-shell nanocrystals, exchange inter-coupling, spin flipping

1. Introduction

Traditionally, the change in free energy that occurs at a constant temperature is attributed to the mechanical work by the system and the magnetic work by the applied magnetic field. The

INTECH
open science | open minds

© 2016 The Author(s). Licensee InTech. This chapter is distributed under the terms of the Creative Commons Attribution License (http://creativecommons.org/licenses/by/3.0), which permits unrestricted use, distribution, and reproduction in any medium, provided the original work is properly cited. CC BY

integral of the magnetic work gives the energy of the magnetization, which is always positive, because work must be done in the system in order for the magnetic field to establish the magnetization. Consequently, in an inverted hysteresis, the so-called proteretic system, the area of the inverted hysteresis loop $\oint HdM$ represents the energy dissipation for each cycle. At the nanoscale, the various temperatures and size of the hysteresis $M(H)$ loop influence the loop direction, such as whether it is counterclockwise (hysteresis) or clockwise (inverted hysteresis). Interestingly, the modulation of hysteresis and inverted hysteresis breaks the conception of the magnetic system [1]. Recently, a clockwise $M(H)$ loop has also been observed in CrO_2/Cr_2O_3 and Co/CoO core-shell particle systems. Zheng et al. [2] observed a series of inverted hysteresis loops between 261 and 292 K in CrO_2 [ferromagnetic (FM)] core particles coated with a Cr_2O_3 [antiferromagnetic (AFM)] surface layer. Wei et al. [3] observed an inverted hysteresis loop in Co (FM) with a core size of 3–4 nm and a CoO (AFM) shell with a thickness of ~3 nm, only giving an example at a temperature T=70 K. When the Co core size is smaller than 3 nm and larger than 4 nm, the $M(H)$ loop leads to an ordinary hysteresis loop. They provided a possible explanation that the proteretic behavior and its size effect dependence reflect the magnetic interaction between various anisotropies and exchange intercouplings in the Co and CoO phases [3]. In another work, Ohkoshi et al. [4] reported the observation of an inverted hysteresis loop that can be reasonably explained by competition between the spin-flip transitions and the uniaxial magnetic anisotropy. The competing anisotropy theory has been extended to systems involving competing cubic and uniaxial anisotropies [5] and two competing uniaxial anisotropies [6]. In the present work dealing with Ni/NiO core-shell nanoparticles, we ignore the influence of intracoupling to simplify the complex interactions and only discuss the intercoupling between Ni core and NiO shell. We design a core-shell anisotropic energy (CSAE) model, tuning the competition between the magnetic anisotropy and exchange intercoupling in the system, to describe the observation of hysteretic and proteretic behaviors in Ni/NiO core-shell nanoparticles. Recently, the tuning of the exchange intercoupling in core-shell magnetic nanocrystals has received intense attention because it allows the control of the interfaces in nanoscale building blocks and inverted hysteresis. The magnetic compositions of core-shell nanocrystals can be selected as FM, AFM, or paramagnetic (PM) materials, so that the exchange intercoupling between them results in a large effective anisotropic energy [7] and intercoupling energy. We also integrate some magnetic models including the Langevin function, the CSAE, and the Stoner-Wohlfarth (SW) model, providing a convenient simulation for the description of the hysteresis and proteresis loops.

2. Stoner-Wohlfarth model

The evolution of the magnetic theory model for the description of the hysteresis loop starts with the SW model [8], which was developed by Edmund Clifton Stoner and Erich Peter Wohlfarth in 1948. The basic hypotheses in this SW model include the following: (a) single-domain particles, (b) spherical geometry, (c) magnetic anisotropy along the easy axis (EA), and (d) non- or weak-interaction between small particles. Additionally, the sources of magnetic anisotropy can be divided into three parts: magnetocrystalline anisotropy, shape anisotropy,

http://dx.doi.org/10.5772/62398

and exchange anisotropy [9]. In the first case, magnetocrystalline anisotropy, the preferential direction for magnetization, arises from the atomic structure of the crystal. In shape anisotropy, it originates from the nonuniform spherical particle shapes, which cause the demagnetizing field to be unequal in all directions, creating one or more EAs. Third, in exchange anisotropy, magnetization originates from the interaction between AFM and FM materials. The SW model is considered to relate to uniaxial magnetic anisotropy, which may originate from magneto-crystalline anisotropy and shape anisotropy. As a magnetic field is applied to a single-domain particle, the moment M of a single-domain particle is subjected to two competing forces: one is due to a uniaxial anisotropy characterized by K toward an EA and the other is due to an external magnetic field H_a, as shown in **Figure 1a**. The total energy is the sum of the anisotropic energy E_A and the Zeeman energy $E_Z = -M \cdot H_a$. At absolute zero T=0 K, the energy is then expressed as

$$E = E_Z + E_A = -MH_a \cos\theta + K \sin^2(\theta - \varphi), \tag{1}$$

where M indicates the saturation magnetization, θ indicates the deviation of M from the field direction, φ indicates the deviation of the corresponding easy axis (EA) from the field direction, and K is the corresponding uniaxial magnetic anisotropy strengths. For the moment, we select an angle θ_m, which is oriented toward either a stable or a bistable state, giving the minimum energy E_m and magnetic field H_f, respectively. The total energy of $E(\theta, H_a)$ may be derived by solving the equations

$$\left(\frac{\partial E}{\partial \theta}\right)_{\theta=\theta_m} = 0 \quad \text{and} \quad \left(\frac{\partial^2 E}{\partial \theta^2}\right)_{\theta=\theta_m} > 0, \tag{2}$$

Moreover, the angle of a magnetic moment dependent on total energy exhibits an energy barrier in a selective applied magnetic field H_a, such as H_a=0, H_a>0, or H_a>H_f, as shown in **Figure 1b**. When the field H_a is zero, the energy barrier exhibits a saddle shape, giving both stable solutions. When the field H_a increases, the energy barrier between the stable and bistable states decreases, implying that the field H_a provides Zeeman energy E_Z to compete with the anisotropic energy E_A. The spin direction in the bistable state gradually becomes more unstable. When the field H_a reaches H_f, the energy barrier between the stable and bistable states disappears. In this condition, the Zeeman energy E_Z is larger than the anisotropic energy E_A. The moment of a single-domain particle will then switch from spin-up to spin-down and orient itself toward the direction of the applied field, giving only one solution. As for the initial state of the magnetic moment M, it will make a choice between the stable and bistable states following a pattern like water flowing downhill. The ideal is to establish a loop process, which can be used to describe a transitional hysteresis loop. Its magnetization can readily be calculated by evaluating $M(H_a)$=$M_s$cosθ_m. Thus, the SW model provides the basis for the description of the hysteresis loop, which can be further extended to a CSAE system.

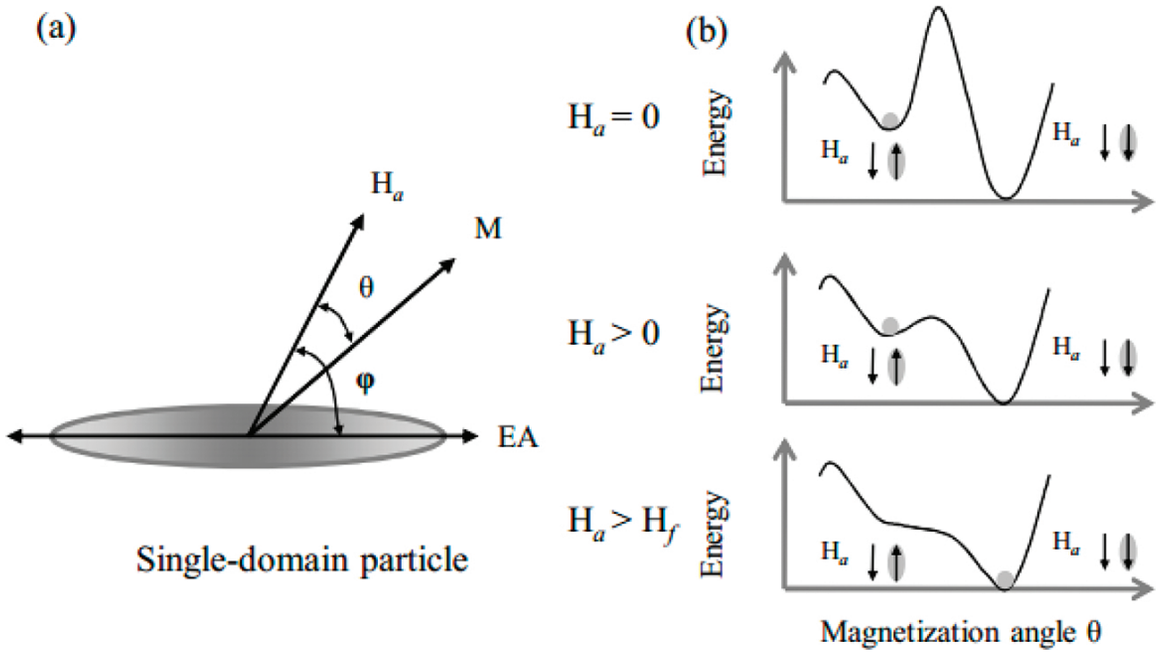

Figure 1. (a) Schematic illustration of a single-domain particle with the magnetic moment (M) and EA under an applied field (H_a). (b) Variation of the energy landscape with angle θ in a selective applied magnetic field, such as H_a=0, H_a>0, and H_a>H_f.

3. Core-shell anisotropic energy model

Neel [10] described the thermal fluctuations of the magnetic moment of a single-domain FM particle and its decay towards thermal equilibrium, neglecting the contribution of magnetic anisotropy. The further development of the thermal activated magnetization is described by the Brown model [11]. Fluctuations in the thermal energy k_BT cause continual changes in the orientation of the moment of an individual nanoparticle. An ensemble of such nanoparticles maintains a distribution of orientation characteristics of statistical equilibrium. The thermal fluctuations are important in superparamagnetism, which can be described by a "Langevin function," providing a description of the thermal activated magnetization. A number of models have been established [12–14] to explain the phenomena of inverted hysteresis for germanium nanostructures [15] and hysteresis for Mackay icosahedral gold nanoparticles [16], using the competing anisotropy model, and based on the SW model [8]. In the case studied here, the general picture of the core-shell system established in the Ni core (FM) coated with a NiO shell (AFM) can be described as two nonidentical phases [17], as shown in **Figure 2a**. Usually, in the macroscopic view, most of the native oxide shells of transition metals (Co, Ni) are either AFM or FM. The magnetism on the FM core has been either neglected or reported to be effective only at low temperatures [18, 19].

http://dx.doi.org/10.5772/62398

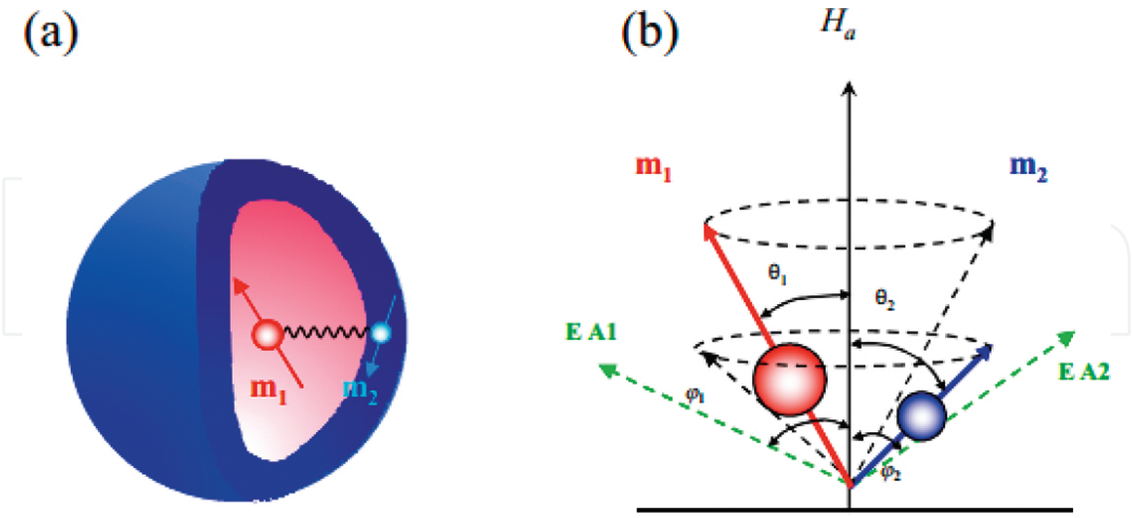

Figure 2. (a and b) Schematic illustration of a core-shell particle with two interacting magnetic moments m_1 and m_2 and EAs EA1 and EA2 under an applied field H_a. They couple at an angle (q_1-q_2) and exchange intercoupling energy E_J between the surface and inner moments.

Because most of the AFM spins are arranged collinearly and the number of sublattices are the same, the resulting magnetization is zero and the coupling vanishes to the first order [20, 21]. However, in the present core-shell system, the existence of correlated magnetic exchange intercoupling between the core-shell moments can be treated as an "exchange spring," which can create an exchange field, inducing a canting of the AFM surface layer that "cannot" be neglected. The interpretation of the occurrence of exchange intercoupling between the surface and the core further indicates that magnetism develops not only in the core atoms but also extends into the surface ones. Treating the surface atoms and the inner atoms gives rise to a net surface macromoment m_2 and a net inner macromoment m_1 that will couple at angles (θ_1-θ_2) and will lead to the development of exchange intercoupling energy E_J between the surface and inner moments. We believe that the associated magnetism is indeed an intrinsic property of Ni/NiO core-shell nanoparticles. The extrinsic factors, such as the shape and temperature, are thus neglected in the considerations of the model. Conducting quantitative analysis of the intercoupling of the core-shell system, and neglecting the contribution of intracoupling, we can express the CSAE E triggered by various magnetic applied fields H_a as

$$E = -m_1 V_1 H_a \cos\theta_1 - m_2 V_2 H_a \cos\theta_2 + k_1 V_1 \sin^2(\theta_1 - \varphi_1) + k_2 V_2 \sin^2(\theta_2 - \varphi_2) + E_J \cos(\theta_1 - \theta_2) \cdot \quad (3)$$

where V_1 and V_2 indicate the volume of the Ni core and NiO shell for each nanoparticle, θ_1 and θ_2 indicate the deviations of m_1 and m_2 from the field direction, φ_1 and φ_2 indicate the deviations of the corresponding EAs from the field direction, and k_1 and k_2 are the corresponding uniaxial magnetic anisotropy strengths, as shown in **Figure 2b**. E_J is defined as $\sigma_{ex} V_s$, where σ_{ex} indicates

the exchange intercoupling energy per area and V_s indicates the interfacial area between the Ni core and NiO shell. The magnetization can readily be calculated by solving $M(H_a)=m_1\cos\theta_{1m} + m_s\cos\theta_{2m}$, where θ_{1m} and θ_{2m} are the θ_1 and θ_2, respectively, that minimize E_m at each H_a. Depending on the relative strength between m_1 and m_2 and between k_1 and k_2, the value of E_J and the bistable energy of $E(\theta_{1m},\theta_{2m},H_a)$ may be derived by solving the following equations: $\partial E/\partial\theta_1=\partial E/\partial\theta_1=0$ [15, 22]. **Figure 3** shows an example of the dependence of the energy E of angles θ_1 and θ_2 on the selection of the applied magnetic field, such as $H_a=0$, $H_a>0$, or $H_a>H_f$, giving a two-dimensional energy barrier. Here, different colors are used to differentiate the energy intensity, with red indicating high energy and purple low energy. When the field H_a is zero, the energy barrier exhibits two whirlpools, indicating stable and bistable solutions. A two-dimensional and high-energy barrier appears between the two whirlpools. With an increase of the field H_a, the energy barrier between the stable and bistable states decreases, implying that the field H_a provides Zeeman energy to compete with the magnetic anisotropies and the exchange intercoupling. The magnetic directions of the core and shell moments in the bistable state gradually become more unstable. When the field H_a reaches H_f, the energy barrier between the stable and bistable states disappears. In this condition, the Zeeman energy is larger than the magnetic anisotropies and the exchange intercoupling. The core and shell moments will switch from bistable to stable states, and the core moment (FM) then becomes oriented toward the applied field direction, giving only one solution. The initial state of the core and shell moments m_1 and m_2 can assume either a stable or bistable state following a pattern like water flowing downhill. Observe the energy barrier along the dashed line in **Figure 4**. The simplified energy barrier clearly exhibits stable and bistable states, which is similar to the SW model. The exchange intercoupling between the core and shell moments in the CSAE model also plays an important role on the $M(H)$ loop process for the modulation of the hysteresis and inverted hysteresis loops. Huang et al. [15] reported the $M(H)$ loop processes and the modulation of the magnetic anisotropies and exchange intercoupling describing proteresis.

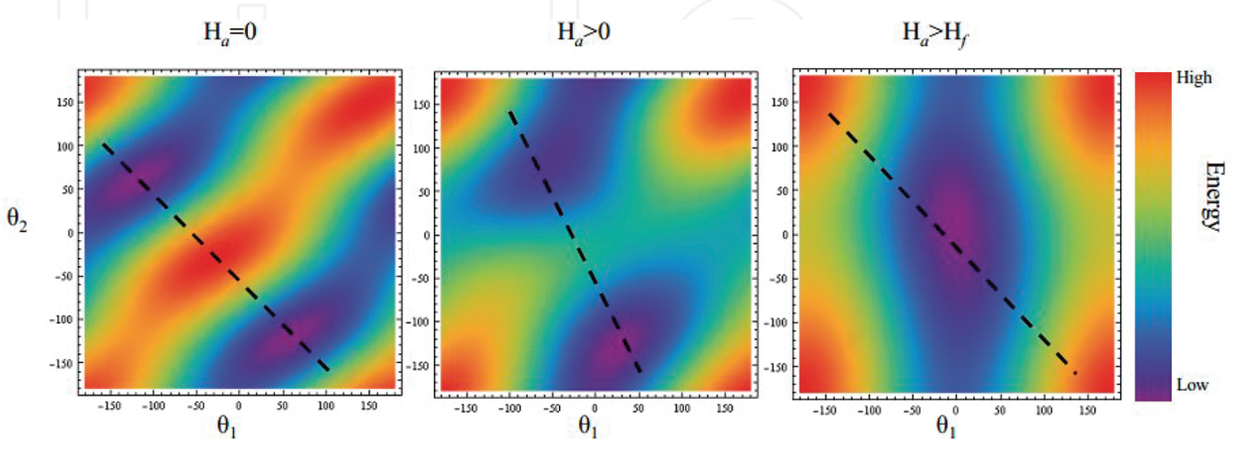

Figure 3. Variation of the energy landscape with angles θ_1 and θ_2 in a selective applied magnetic field, such as $H_a=0$, $H_a>0$, and $H_a>H_f$, giving a two-dimensional energy barrier.

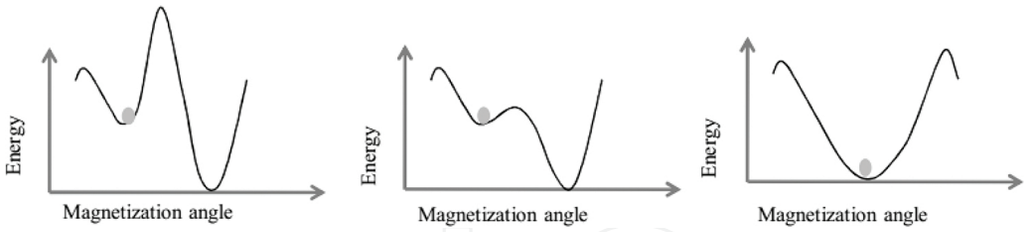

Figure 4. Observation of the energy barrier along the dashed line (**Figure 3**) clearly shows the stable and bistable states in the one-dimensional energy barrier.

4. Spin dynamics

In the Ni/NiO core-shell nanoparticle system, treating the inner Ni atoms and surface NiO atoms gives rise to a net inner macromoment m_1 and a net surface macromoment m_2. The strength of the exchange intercoupling $E_J=\sigma_{ex}V_s$ is between the two moments of m_1 and m_2. Moreover, the fluctuation in the thermal energy $k_BT\neq0$ causes continual changes in the orientation of the moment of an individual nanoparticle, giving a thermally activated magnetization. Thus, to provide good simulation results, the magnetic model of the Ni/NiO core-shell nanoparticle system requires combining the CSAE model with the Langevin function. **Figure 5** shows an example of the field dependence of the magnetization. The inverted hysteresis for the 13.9(2) nm sample appears at T=150 K. The black open circles (experimental data) can be described by a magnetic model with a blue line (decreasing field) and a red line (increasing field). An examination of the bottom of **Figure 5** shows the process of spin dynamics from H_a=1 kOe to H_a=-1 kOe, indicating a decreasing field. In the field H_a=1 kOe, the Ni core moment m_1 is toward the field direction, showing coupling at an angle $|\theta_1-\theta_2|$=88.3° between m_1 (red line) and m_2 (blue line). When the field decreases to zero, the m_1 magnetization along the vertical direction component decreases, and the coupling angle between m_1 and m_2 increases to $|\theta_1-\theta_2|$=172.8°. As the field decreases to H_a=-1 kOe, the Ni core moment m_1 moves toward the negative field direction, and the coupling angle decreases to $|\theta_1-\theta_2|$=115.6°. For an increasing field, the process of spin dynamics is similar to the results for a decreasing field, but the directions of m_1 and m_2 at H_a=1 kOe are not the same. The explanation is that one solution is still in a bistable state. Thus, the field H_a has a great impact on the coupling angle between m_1 and m_2. For the $M(H)$ loop direction, the parameters in the simulation, $m_1>m_2$, $k_1<k_2$, and $E_J\neq0$, apply to the description of inverted hysteresis in the low field. In the higher field, the exchange intercoupling between m_1 and m_2 will be destroyed by the Zeeman energy, which changes the $M(H)$ loop direction to counterclockwise. A similar $M(H)$ loop has been reported in a germanium nanostructure system [15]. The exchange intercoupling strength E_J between the core and shell plays an important role in guiding the direction of the $M(H)$ loop. If there is no interaction between the core and shell moments, the $M(H)$ loop only exhibits hysteresis. If the exchange intercoupling strength E_J is larger than the magnetic anisotropies KV, the binding energy between m_1 and m_2 can be treated as a single nanoparticle system, giving rise to the hysteretic behavior. When the exchange intercoupling strength E_J is comparable to the magnetic anisotropy K_1V_1 or K_2V_2, the $M(H)$ loop will be guided to be proteretic.

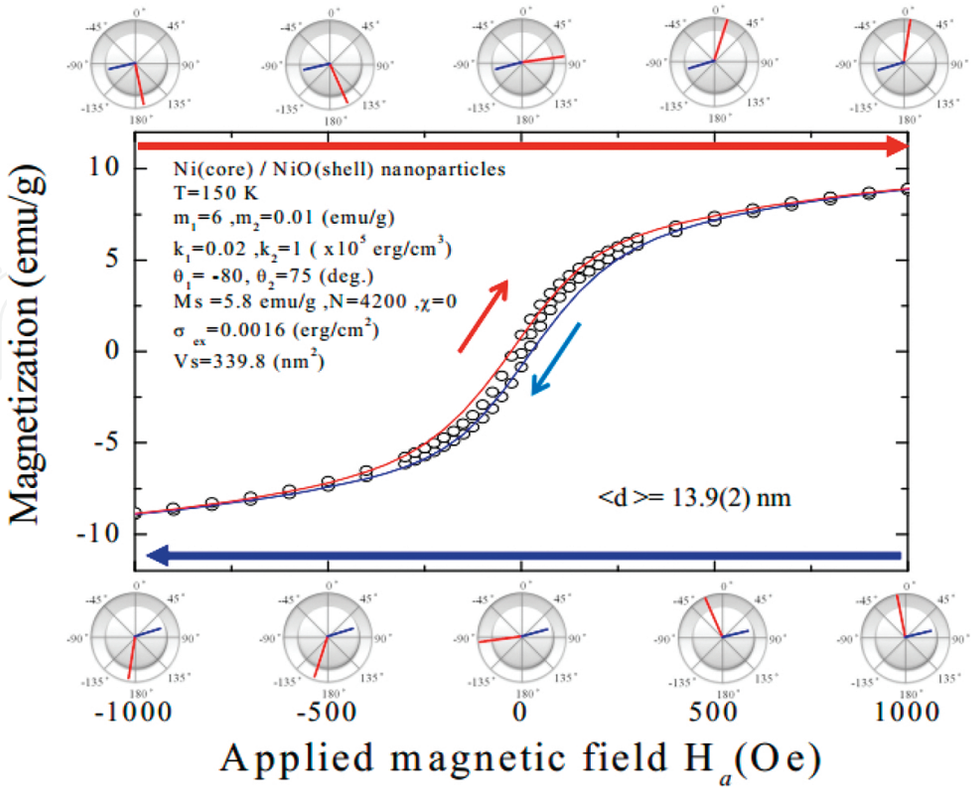

Figure 5. Field dependence of the magnetization, giving an example of inverted hysteresis for the 13.9(2) nm sample at T=150 K. The black circle (experimental data) can be described by a magnetic model with a blue line (decreasing field) and a red line (increasing field).

In the example illustrated in **Figure 5**, the parameters used in the simulation, $E_J=\sigma_{ex}V_s$=3.4 meV, K_1V_1=0.74 meV, and K_2V_2=51 meV, give a proteretic loop, which corresponds to the above description. In terms of the spin dynamics, the angles θ_1 and θ_2 for each field provide spin processes that lead to an increasing field, as shown in **Figure 6a**, and a decreasing field as shown in **Figure 6b**. The CSAE simulation produces proteretic behavior in the 13.9(2) nm sample after solving the spin dynamics for the decreasing field and increasing field. This result suggests that the spin-orientation results in proteretic behavior. Applying the process-dependent summary of angles θ_1 and θ_2, we consider a decreasing-field process below and above the blocking temperature T_B for two selected samples [<d>=7.2(3) nm and 19.0(2) nm], as shown in **Figures 7** and **8**. **Figure 7** shows the spin processes for the decreasing field for angles θ_1 and θ_2 in the 7.2(3) nm sample. Two examples of the field-dependent spin dynamics at temperatures below and above T_B=20 K, T=2 K, and T=50 K, respectively, are given. The spin dynamics exhibit a spin-flip for the angle θ_1 at T=2 K and spin-orientation at T=50 K for the angle θ_1, implying a change of the Ni core moment m_1. However, the phenomenon of spin-orientation was not found in the 19.0(2) nm sample, as shown in **Figure 8**, where the temperature is above the blocking temperature. Based on the observed field-dependent spin dynamics for T=2 K to T=300 K, we give a summary of the region for spin-flip (white region) and spin-orientation (gray region), which corresponds to the distinction between hysteresis and proteresis (see **Figure 9**). The phase diagram of the spin dynamics implies a limit of the

http://dx.doi.org/10.5772/62398

proteretic behavior and spin-orientation below a mean size of <*d*>=15.8 nm, which indirectly indicates a limit to the magnetic instability in the Ni (FM) core particles coated with NiO (AFM) shells. It also reveals the reason why there is no proteresis when the mean size is large. Controlling the proteretic behavior requires a mean size below <*d*>=15.8 nm and temperature above T_p. The proteretic behavior relates to the spin-orientation, which has a rotation along EA. This will cause the destruction of the magnetic record. The result helps us to understand the limitations of recording data for the Ni/NiO core-shell nanoparticles on the size effect, which will affect the development of the magnetic industry in the future.

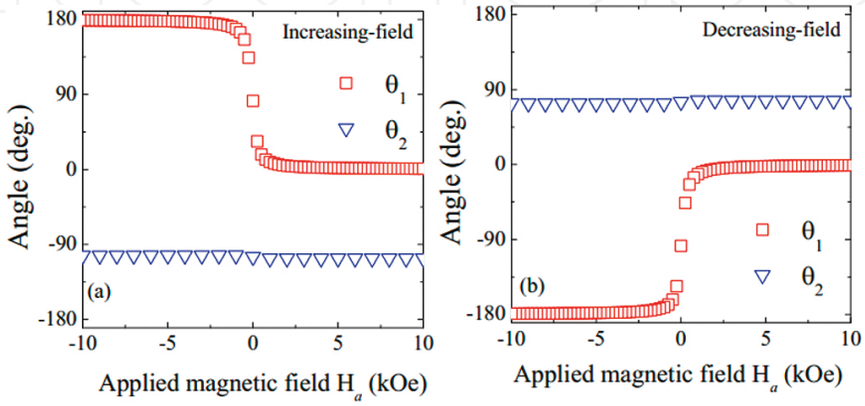

Figure 6. Simulation results provide a possible solution to elaborate spin dynamics for (a) the increasing field and (b) the decreasing field in the Ni/NiO core-shell nanoparticles.

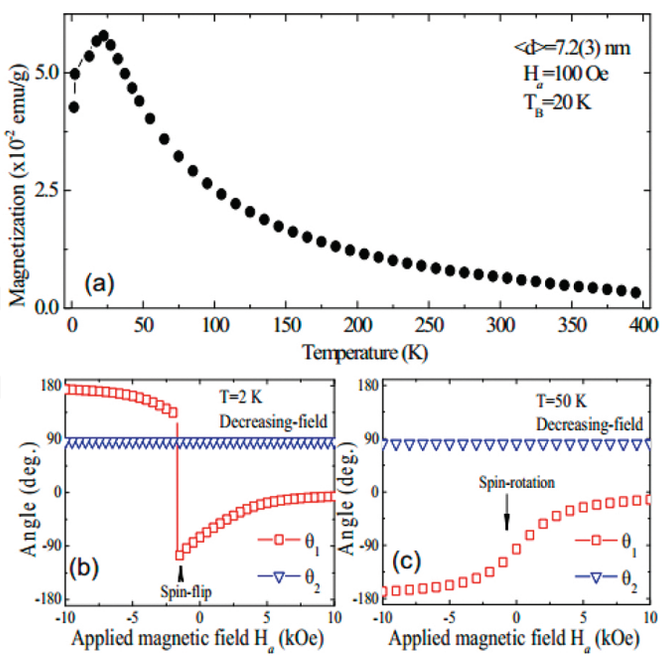

Figure 7. (a) Temperature dependency of magnetization. (b and c) Magnetic field-dependent summary of the angles θ_1 and θ_2 for the decreasing-field process below (T=2 K) and above (T=50 K) the blocking temperature T_B for <*d*>=7.2(3) nm sample.

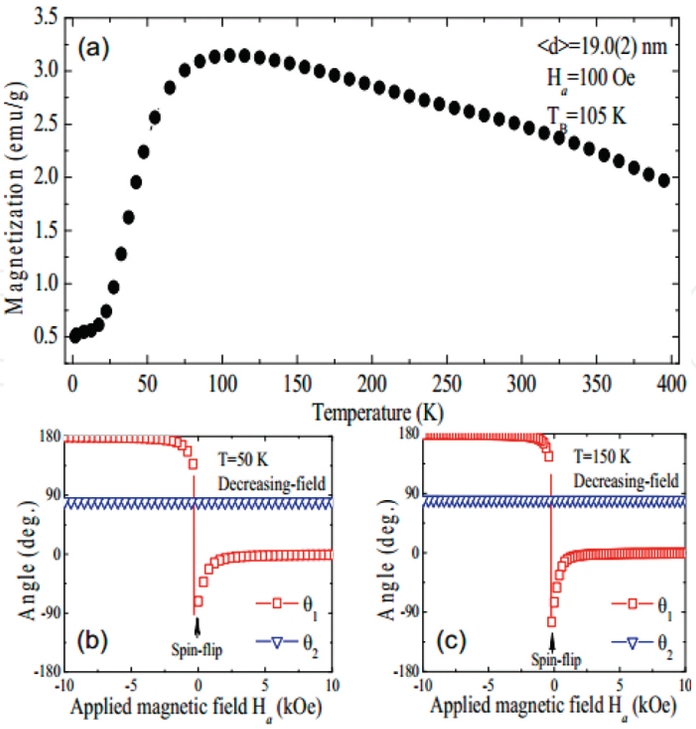

Figure 8. (a) Temperature dependence of magnetization. (b and c) Magnetic field-dependent summary of the angles θ_1 and θ_2 for the decreasing-field process below (T=50 K) and above (T=150 K) the blocking temperature T_B for the <d>=19.0(2) nm sample.

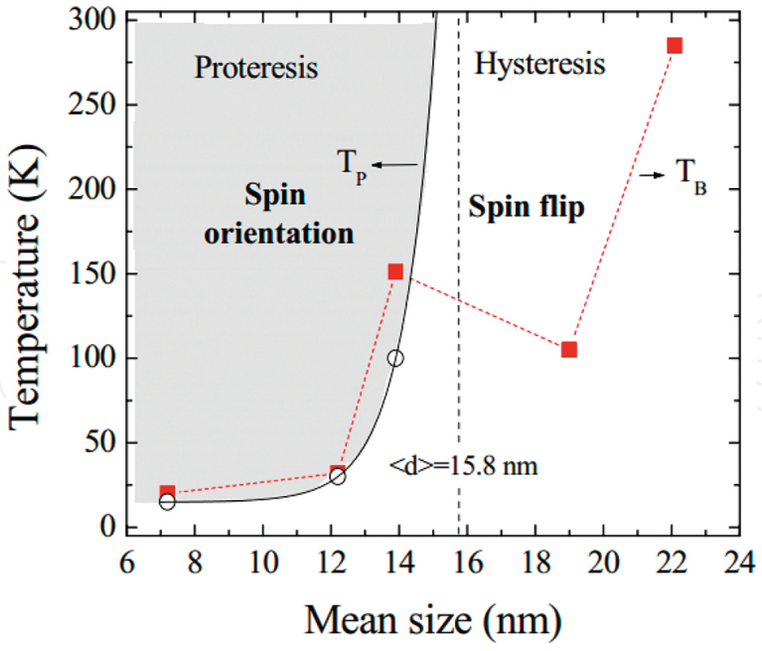

Figure 9. Summary of the $M(H)$ loop direction for hysteresis and proteresis at a series of temperatures for each sample and resulting spin-flip or spin-orientation.

5. Conclusion

Analysis of the results leads to some interesting conclusions. First, the impact of the size effect on the temperature-dependent $M(H)$ loop allows the modulation of hysteresis and proteresis, which breaks the concept of a magnetic system. The $M(H)$ loop between hysteresis and proteresis can be distinguished through analysis of the difference in magnetization ΔM, giving a summary of T_p, which results in an appearance of the proteretic behavior. In addition, we design a CSAE model, tuning the competition between magnetic anisotropy and exchange intercoupling, to describe the observation of hysteretic and proteretic behaviors in Ni/NiO core-shell nanoparticles. The CSAE simulation results show how the spin dynamics in the hysteresis and proteresis loops give rise to a spin-flip and spin-orientation, respectively. Finally, the phase diagram of the spin dynamics suggests a limit to the proteretic behavior and spin-orientation below a mean size of $<d>$=15.8 nm, which indirectly indicates a limit to the magnetic instability of Ni (FM) core particles coating the NiO (AFM) shells. It also explains why no proteresis occurs when the mean particle size is large. Controlling the proteretic behavior requires a mean particle size below $<d>$=15.8 nm and temperature above T_p. Finally, the results of magnetic analysis help us to understand the limitations of recording data for the Ni/NiO core-shell nanoparticles on the size effect, which will have implications for the development of the magnetic industry in future.

Acknowledgements

We would like to thank the Ministry of Science and Technology (MOST) of the Republic of China for their financial support of this research through project numbers MOST-103-2112-M-259-005 and MOST-104-2112-M-259-001.

Author details

Jhong-Yi Ji and Sheng Yun Wu*

*Address all correspondence to: sywu@mail.ndhu.edu.tw

Department of Physics, National Dong Hwa University, Taiwan

References

[1] Wu SY, Ji J-Y, Shih P-H, Gandhi AC, Chan TS. Proteresis of Cu_2O/CuO core-shell nanoparticles: Experimental observations and theoretical considerations. J Appl Phys 2014;116:193906. DOI: 10.1063/1.4902524s.

[2] Zheng RK, Liu H, Wang Y, Zhang XX. Inverted hysteresis in exchange biased Cr_2O_3 coated CrO_2 particles. J Appl Phys 2004;96:5370–5372. DOI: 10.1063/1.1795983

[3] Wei XH, Skomski R, Sun ZG, Sellmyer DJ. Proteresis in Co:CoO core-shell nanoclusters. J Appl Phys 2008;103: 07D514. DOI: 10.1063/1.2829239.

[4] Ohkoshi SI, Hozumi T, Hashimoto K. Design and preparation of a bulk magnet exhibiting an inverted hysteresis loop. Phys Rev B 2001;64:132404. DOI: 10.1103/PhysRevB.64.132404.

[5] Geshev J, Viegas ADC, Schmidt JE. Negative remnant magnetization of fine particles with competing cubic and uniaxial anisotropies. J Appl Phys. 1998;84:1488–1492. DOI: 10.1063/1.368214.

[6] Valvidares SM, Alvarez-Prado LM, Martin JI, Alameda JM. Inverted hysteresis loops in magnetically coupled bilayers with uniaxial competing anisotropies: Theory and experiments. Phys Rev B 2001;64:134423. DOI: 10.1103/PhysRevB.64.134423.

[7] Gao Y, Shindo D, Bao Y, Krishnan K. Electron holography of core-shell Co/CoO spherical nanocrystals. Appl Phys Lett 2007;90:233105. DOI: 10.1063/1.2747052.

[8] Stoner EC, Wohlfarth EP. A mechanism of magnetic hysteresis in heterogeneous alloys. Philos Trans A 1948;240:599–642. DOI: 10.1098/rsta.1948.0007.

[9] Schüler K. McCaig: Permanent magnets in theory and practice. Physikalische Blätter 1979;35:423. DOI: 10.1002/phbl.19790350913.

[10] Neel LCR. Influence des fluctuations thermiques sur l'aimantation de grains ferromagnetiques tres fins. Acad Science (Paris), Series B 1949; 228 : 664–666.

[11] Brown WF. Thermal fluctuations of a single-domain particle. Phys Rev 1963;130:1677. DOI: 10.1103/PhysRev.130.1677.

[12] Gao C, O'Shea MJ. Inverted hysteresis loops in CoO-based multilayers. J Magnet Magnet Mater 1993;127:181–189. DOI: 10.1016/0304-8853(93)90213-L.

[13] Thiaville A. Coherent rotation of magnetization in three dimensions: A geometrical approach. Phys Rev B 2000;61:12221–12232. DOI: 10.1103/PhysRevB.61.12221.

[14] Wernsdorfer W. Classical and quantum magnetization reversal studied in nanometer-sized particles and clusters. Adv Chem Phys 2007;118:99–190. DOI: 10.1002/9780470141786.

[15] Huang YL, Wang HL, Chan KC, Wu SY, Wong MS, Yeh SF, Lin CI. Size-effect induced short-range magnetic ordering in germanium nanostructures. J Nanosci Nanotechnol 2010;10:4629–4634. DOI: 10.1166/jnn.2010.1698.

[16] Wu CM, Li CY, YT Kuo, Wang CW, Wu SY, Li W-H. Quantum spins in Mackay icosahedral gold nanoparticles. J Nanoparticles Res 2010;12:177–185. DOI: 10.1007/s11051-009-9592-3.

[17] Ji J-Y, Shih P-H, TS Chan, Ma Y-R, Wu SY. Magnetic properties of cluster glassy Ni/NiO core-shell nanoparticles: An investigation of their static and dynamic magnetization. Nanoscale Res Lett 2015;10:243. DOI: 10.1186/s11671-015-0925-0.

[18] Sharrock MP. Recent advances in metal particulate recording media: Toward the ultimate particle. IEEE Trans Magnet 2000;36:2420–2425. DOI: 10.1109/20.908453

[19] Nogues J, Sort J, Langlais V, Skumryev V, Surinach S, Munoz JS, Baro MD. Exchange bias in nanostructures. Phys Rep 2005;422:65–117. DOI: 10.1016/j.physrep.2005.08.004.

[20] Fröbrich P, Kuntz PJ, Jensen PJ. Coupled ferro-antiferromagnetic Heisenberg bilayers investigated by many-body Green function theory. J Phys Condensed Matter 2005;17:5059. DOI: 10.1088/0953-8984/17/33/010.

[21] Jensen PJ, Dreyssé H, Kiwi M. Magnetic reordering in the vicinity of a ferromagnetic/antiferromagnetic interface. Eur Phys J B 2005;46;541–551. DOI: 10.1140/epjb/e2005-00287-y.

[22] Xu C, Li ZY, Hui PM. Monte Carlo studies of hysteresis curves in magnetic composites with fine magnetic particles. J Appl Phys 2001;89:3403. DOI: 10.1063/1.1348326.

IntechOpen

IntechOpen

IntechOpen